Title: Protein Vaccine Induces a Durable, More Broadly Neutralizing Antibody Response in Macaques than Natural Infection with SARS-CoV-2 P.1

Authors: Albert To[1], Teri Ann S. Wong[1], Michael M. Lieberman[1], Karen Thompson[2], Laurent Pessaint[3], Jack Greenhouse[3], Nisrine Daham[3], Anthony Cook[3], Brandon Narvaez[3], Zack Flinchbaugh[3], Alex Van Ry[3], Jake Yalley-Ogunro[3], Hanne Andersen Elyard[3], Chih-Yun Lai[1], Oreola Donini[4], Axel T. Lehrer[1*]

Affiliations:

[1]Department of Tropical Medicine, Medical Microbiology, and Pharmacology, John A. Burns School of Medicine, University of Hawai'i at Mānoa, Honolulu, HI, USA

[2]Department of Pathology, John A. Burns School of Medicine, University of Hawai'i at Mānoa, Honolulu, HI, USA

[3]Bioqual Inc., Rockville, MD, USA

[4]Soligenix, Inc, Princeton, NJ, USA

*Corresponding author at: Axel T. Lehrer: (lehrer@hawaii.edu). University of Hawai'i at Mānoa, John A. Burns School of Medicine, Department of Tropical Medicine, 651 Ilalo Street, Honolulu, HI 96813, United States

One Sentence Summary: A recombinant subunit protein formulated with CoVaccine HT™ adjuvant induces superior immunity than natural infection and reduces viral load while protecting cynomolgus macaques from COVID-19-like disease caused by late SARS-CoV-2 P.1 (Gamma) challenge.

Abstract: FDA-approved and Emergency Use Authorized (EUA) vaccines using new mRNA and viral-vector technology are highly effective in preventing moderate to severe disease, however, information on their long-term efficacy and protective breadth against SARS-CoV-2 Variants of Concern (VOCs) is currently scarce. Here we describe the durability and broad-spectrum VOC immunity of a prefusion-stabilized spike (S) protein adjuvanted with liquid or lyophilized CoVaccine HT™ in cynomolgus macaques. This recombinant subunit vaccine is highly immunogenic and induces robust spike-specific and broadly neutralizing antibody responses effective against circulating VOCs (B.1.351 [Beta], P.1 [Gamma], B.1.617 [Delta]) for at least 3 months after the final boost. Protective efficacy and post-exposure immunity were evaluated using a heterologous P.1 challenge nearly 3 months after the last immunization. Our results indicate that while immunization with both high and low S doses shorten and reduce viral loads in the upper and lower respiratory tract, a higher antigen dose is required to provide durable protection against disease as vaccine immunity wanes. Histologically, P.1 infection causes similar COVID-19-like lung pathology as seen with early pandemic isolates. Post-challenge IgG concentrations were restored to peak immunity levels and vaccine-matched and cross-variant neutralizing antibodies were significantly elevated in immunized macaques indicating an efficient anamnestic response. Only low levels of P.1-specific neutralizing antibodies with limited breadth were observed in control (non-vaccinated but challenged) macaques suggesting that natural infection may not prevent reinfection by other VOCs. Overall, these results demonstrate that a properly dosed and adjuvanted recombinant subunit vaccine can provide long-lasting and protective immunity against circulating VOCs.

Main Text:

INTRODUCTION

COVID-19 is a respiratory disease caused by the Severe Acute Respiratory Syndrome Coronavirus 2 (SARS-CoV-2) (*1, 2*) and is commonly characterized as an asymptomatic

infection or a self-limiting, febrile illness co-presenting with cough, shortness of breath, and fatigue (*3, 4*). Severe complications can result in approximately 6-10% of infected patients (*5*) developing pneumonia, acute respiratory distress syndrome, multi-organ dysfunction and arterial thromboembolic events that can result in hospitalization and/or death (*6-9*). Transmission occurs through respiratory droplets during close contact with asymptomatic or presymptomatic infected individuals (*10-12*). The synergistic relationship between the infectivity and high transmissibility with low virulence has contributed to the ongoing global public health crisis, and the emergence of more transmissible and potentially more pathogenic variants of concern (VOCs). Longitudinal cross-sectional studies have indicated only a fraction of asymptomatic to mild and moderate SARS-CoV-2 natural infections of humans results in detectable neutralizing antibodies months after recovery (*13-15*) and current evidence suggests that convalescent immunity may only provide transient protection (*16-18*). Furthermore, the degree of immune evasion witnessed *in vitro* by spike (S) protein variants and the increasing occurrence of reinfection (*19-23*) has raised the question whether previous infection or vaccine-derived immunity can provide heterologous protection against further transmission and limit additional mutation of circulating VOC, even while protection against severe disease and mortality has been sustained to date.

Some VOCs show increased transmissibility, cause more severe disease than original strains and demonstrate greater immune evasion to neutralizing antibodies as they harbor mutations at sites facilitating viral fusion (*24, 25*) and at critical epitopes in the N-terminal (NTD) and receptor binding domains (RBD). The B.1.1.7 (Alpha), B.1.351 (Beta) and P.1 (Gamma) variants contain the same set of mutations, K417T, E484K, and N501Y, while the B.1.617 (Delta) carries L452R and T478K mutations, all of which are associated with enhanced infectivity and reduced serum neutralization (*26-28*). These antigenic changes have abolished potent neutralizing epitopes targeted by monoclonal antibody therapeutics (*29*) and antibodies elicited by mRNA vaccination

(*30*). Natural reinfection with the VOC strains after original strain infection, and *vice versa*, has been documented (*20, 31-34*). Despite this, cross-neutralization of convalescent sera from patients infected with non-variants and mRNA immunized individuals suggests that the parental spike (S) protein in current vaccines affords some degree of protection (*35-37*).

Phase 1-3 clinical trials of novel mRNA (Moderna mRNA-1273 and Pfizer-BioNTech BNT162b2) and viral-vector (Johnson & Johnson-Janssen Ad26.COV2.S) platform, utilizing the original Wuhan-Hu-1 S protein (*38-40*), have shown these vaccines to be highly protective with 94-95% and 67% efficacy against COVID-19 disease, respectively (*41-43*), and they all elicit uniformly high protection against severe disease/death (i.e., >85%). Post-hoc sequencing during clinical trials of these and other vaccine platforms in variant-dominant regions have revealed a slightly lower efficacy against B.1.1.7 and B.1.351 variants, albeit usually remaining above the 50% protection threshold (*44, 45*). Attempts at predicting protection based on immune correlates, such as cross-neutralizing antibodies, have shown that vaccinated individuals had a 2 to 5-fold reduction in titers against current VOCs as IgG levels wane, which are nonetheless believed to confer a degree of resistance against infection (*46-49*). However, these samples were taken during the peak period of the humoral response and may not be accurate predictors of protection months onwards when the likelihood of infection is greater. Thus, understanding the decay in antibody responses months after the final boost is an essential endpoint in vaccine development.

Evaluating a delayed vaccine response in non-human primate (NHP) models can provide valuable foresight into the relationship between waning immunity and protection, especially against VOCs. In this study, we describe the immunogenicity and protective efficacy of a recombinant pre-fusion spike subunit (based on the reference SARS-CoV-2 strain, Wuhan-Hu-1) adjuvanted with liquid or lyophilized (dry) CoVaccine HT™, a squalane-in-water

nanoemulsion adjuvant containing immunostimulatory sucrose fatty acid sulfate esters (*50*), in cynomolgus macaques. Other investigators have shown that infection with SARS-CoV-2 (prototype strain) produced COVID-19-like disease in this species and reflects similar viral shedding kinetics and lung pathology as human infections (*51, 52*). We have previously demonstrated that our vaccine candidate elicits a broad-spectrum IgG response including high neutralizing antibody (NtAb) titers against the prototypic SARS-CoV-2 and VOCs, specifically B.1.351 and P.1, and an *in vitro* antigen-specific IFN-γ secreting response from immune splenocytes taken from Swiss Webster mice (*53*). To elaborate on our understanding of the elicited immunological response, we assessed the vaccine efficacy using a delayed challenge scheme with the P.1 VOC to delineate how the maturation and/or decay of the humoral response affects protection from a heterologous SARS-CoV-2 strain. Neutralizing antibody responses to the vaccine-matched WA1/2020 strain, and VOCs, B.1.351, P.1 and B.1.617 were also determined just prior to challenge and 14 days post-challenge (to assess anamnestic responses). Furthermore, we characterize the viral kinetics and histopathological changes post-challenge in the lower and upper respiratory tracts of control (non-vaccinated, challenged), and protected NHPs. To our knowledge, this is the first published account of P.1 VOC challenge in NHPs.

RESULTS

Spike antigen with either liquid or lyophilized CoVaccine HT™ elicits a durable humoral response

Twelve Cynomolgus macaques were assigned into four groups and received two immunizations with 5 (Group A) or 25 (Group B and C) µg liquid prefusion spike trimer (S) antigen formulated with either lyophilized (Group A and C) or liquid (Group B) CoVaccine HT™ adjuvant, or one dose of a co-lyophilized CoVaccine HT™-adjuvanted control containing an unrelated viral glycoprotein antigen (Group D) (Fig. 1A). The two doses were administered within a three-week

interval and all NHPs were challenged with the P.1 isolate 12 weeks post-boost (~ 3 months, study week 15). Wuhan-Hu-1 S- and RBD-specific IgG titers were measured by a multiplexed microsphere immunoassay (MIA) using insect cell expressed antigens coupled onto spectrally distinct, magnetic beads as described previously (*53*). Serum S-specific IgG concentrations were interpolated using a standard curve generated from S-specific human IgG purified from vaccinated individuals (Fig. 1B). RBD-specific IgG titers were read out as median fluorescence intensity (MFI) (Fig. S1). All NHP immunized with the adjuvanted S at both antigen doses seroconverted after the prime (week 3) with S-specific antibodies in the range of 20 to 70 µg/mL, and peak serum IgG concentrations detected two weeks after the boost (week 5) in the range of 70 to 753 µg/mL. Macaques given a 25 µg dose of S demonstrated a greater IgG response to the antigen compared to those receiving 5 µg. RBD-specific IgG titers followed a similar trend. As expected, animals in group D receiving an unrelated antigen did not develop any detectable S-specific IgG during this phase of the study. S-specific IgG remained detectable 12 weeks after the boost (week 15) although IgG concentrations dropped 3.0 to 9.9-fold relative to the prior peak titer.

The titer of NtAb against the prototype WA1/2020 strain was determined using a standard PRNT with wild-type virus (Fig. 1C). NtAb from one animal in Group C was detectable after the prime (week 3). All S-immunized NHPs developed a potent neutralizing response, peaking two weeks after the boost (week 5) and generally remaining stable one week later (week 6). The group receiving 5 µg of the antigen showed the greatest variability. Nearly all immunized NHPs maintained neutralization capacity, with $PRNT_{50}$ greater than 1:150 dilution, 12 weeks after the final immunization (week 15). NtAbs from groups receiving 25 µg S either remained stable or decreased up to 3.0-fold, while the group receiving 5 µg S declined ~2.9-9.2-fold. A similar reduction in serum neutralization was also verified using a surrogate rVSV-SARS-CoV-2 S PRNT assay (Fig. S2).

157

158 **A recombinant subunit vaccine induces stable neutralizing antibodies against VOCs**

159 Circulating SARS-CoV-2 VOCs can evade vaccine-induced antibody responses and are
160 associated with breakthrough infections in those fully immunized, especially as antibody titers
161 wane (*54-60*). To determine whether an adjuvanted, prototypic Wuhan-Hu-1 S subunit can
162 generate durable cross-variant neutralizing antibodies, PRNTs using WT B.1.351, P.1, and
163 B.1.617 isolates were determined with sera collected at the time of peak neutralization and 12
164 months after the final immunization, a timepoint at which antibody titers are expected to have
165 waned. At week 6, potent neutralization of the B.1.351, P.1 and B.1.617 VOC was detected,
166 although 10.7-, 10.7- and 5.7-fold lower, respectively, compared to WA1/2020 in all vaccine
167 groups (Fig. 2A). As antibody titers waned 10 weeks later (study week 15) the gap between
168 neutralization titers against the WA1/2020 strain to the VOC isolates narrowed to a 4.5-, 6.3-
169 and 5.1-fold difference (Fig. 2B) driven by a proportionally larger decline in WA1/2020-specific
170 neutralizing activity. At this later time point, all S-immunized macaques, except for a single
171 macaque in Group A, maintained a detectable $PRNT_{50}$ titer greater than 1:40 dilution. A few
172 macaques in Groups B and C demonstrated greater VOC neutralization at week 15 compared
173 to week 6, suggesting a refinement or “maturation” of the humoral response towards
174 neutralizing epitopes during this interval.

175

176 **Immunization with recombinant subunits reduces viral burden from delayed P.1 (Gamma)**
177 **challenge**

178 The characterization of the prototype strain and B.1.351 variant infections in NHP models has
179 been described previously (*51, 52, 61-63*). Here we characterize the clinical signs and
180 histological events of a P.1 VOC infection in cynomolgus macaques and determine whether a
181 prefusion spike subunit formulated with CoVaccine HT™ is effective at reducing viral load
182 against a circulating VOC after a 12-week interval following the final immunization. All NHPs

were challenged with a total of $1x10^6$ $TCID_{50}$ of the P.1 isolate using simultaneous intranasal and intratracheal inoculation routes. None of the NHPs challenged developed visible clinical signs of respiratory disease throughout the study, consistent with WA1/2020 strain infected cynomolgus macaques (*51*). Bronchioalveolar lavages (BAL) from the lower respiratory tract, and nasal and oral swabs (NS and OS respectively) from the upper respiratory tract were collected at days 2, 4, 7, 10 and 14 after challenge to detect infectious virus, genomic RNA or signs of viral replication. High levels of infectious virus, GMT Log_{10} $TCID_{50}$ titer of 5.8 and 4.8, were recovered two days post-challenge from the NS and BAL, respectively, from control macaques (Group D, Fig. 3A & 3D and S3A-B). Infectious virus continued to be detectable in both anatomic sites until at least day 7 post-challenge before becoming undetectable on day 10. All S-immunized NHPs presented $TCID_{50}$ titers at least 1-2 Log_{10} lower than control macaques in both locations at all timepoints throughout the study, indicating protection conferred by both 5 and 25 µg S formulations of the subunit vaccine. No infectious virus could be cultured from the BAL in S-immunized macaques by day 7. Infectious virus from the NS was recoverable from immunized macaques throughout the study period and was variable between groups, however these macaques on average had $TCID_{50}$ at least 1-2 Log_{10} below those of control animals.

Quantitative RT-PCR was used as an additional measurement for viral load. We detected the presence of viral RNA and viral replication throughout the 14-day study period in both the lower (Fig 3B-C, S4A-C and S5A-C) and upper (Fig 3E-F, S4D-F and S5D-F) respiratory airways and from the oral cavity (Fig 3G-H, S4G-I and S5G-I). Quantification of viral RNA showed that both 5 and 25 µg immunization had reduced the viral load by approximately 1-2 Log_{10} RNA copies/mL (or swab) over Group D macaques, corroborating the $TCID_{50}$ results. Virus replication in the oral cavity was undetectable at least 3 days earlier in most S-immunized macaques than in the control group, suggesting a reduced potential for transmission. High levels of viral RNA and replication, between 5-6 Log_{10} vgRNA and sgRNA copies/mL, respectively, were observed in

these control macaques before gradually resolving at day 10. Altogether, reduced viral loads at all tested anatomic locations in Groups A, B and C macaques indicate a degree of durable protection from P.1 VOC infection provided by an adjuvanted protein subunit vaccine.

High dose spike antigen reduces lung histopathology caused by P.1 (Gamma) challenge

Also consistent with previous prototype virus infection studies in cynomolgus macaques (*51, 52*), P.1 challenge did not cause changes in weight, temperature nor demonstrate any observable signs of respiratory disease. To evaluate vaccine efficacy against COVID-19-like pathology, a section slide from each lung lobe and the bronchi was prepared from each macaque and stained with hematoxylin and eosin to survey for histopathological changes indicative of acute lung injury. The histopathological scoring system based on the presence/severity of edema, intraalveolar and interstitial inflammation, perivascular lymphocytic cuffing, and increased bronchiolar-associated lymphoid tissue (BALT) is outlined in Table S1. A cumulative average score was determined for each macaque based on the evaluation of these five characteristics per section for a total of 30 scores (Fig 4A). Significant differences in the cumulative average scores for each vaccine formulation vs. controls were determined using a one-way ANOVA followed by a Dunnett's multiple comparison test. Macaques in the control Group D appeared to have developed mild to moderate respiratory disease. The lower cumulative GMT scores of Groups B and C, immunized with 25 μg S, suggests that these animals, except for a single macaque, were completely protected from lung pathology while all Group A (immunized with 5 μg S) macaques appeared to have developed mild disease despite exhibiting lower viral loads. Week 15 WA1/2020 NtAb levels were determined to be inversely correlated, although weakly, with histopathology scores using a Spearman's correlation test ($r=-0.682$, $p=0.0178$) (Fig. 4B). Week 15 pre-challenge neutralizing antibody levels were lower in animals with higher histopathology scores, a trend seen with breakthrough infections in fully immunized individuals (*64*). The moderate disease seen in the control animals is demonstrated

in Fig. 5A, where a representative, low-power magnification shows a distribution of lymphocytic perivascular cuffing and clusters of intraalveolar macrophages. In contrast, immunized animals (especially those receiving the higher antigen dose), appeared to have milder disease without these pathological changes (Fig. 5B). Macaques developing mild to moderate disease exhibited absent to moderate, focal and multifocal edema and perivascular cuffing with marked lymphocytic infiltration (Figs. 6A-D). Syncytia of intraalveolar multinucleated giant cells surrounded by acute and eosinophilic inflammatory infiltrate (Fig. 6A.) or increased intraalveolar macrophages with interstitial lymphocytic inflammation, in addition to alveolar septal thickening and complete perivascular cuffing can be seen in a moderately diseased, control macaque (Fig. 6B-C). Proteinaceous edema fluid filling alveolar spaces was also observed in unprotected macaques (Fig. 6D). While these histopathological changes were also noticed in protected macaques, the findings appeared less severe (Fig. 6E-F). A section from a protected macaque revealed a few intraalveolar multinucleated giant cells without an increase in intraalveolar macrophages, lymphocytic vascular cuffing, or interstitial inflammation (Fig. 6E). Similarly, only partial lymphocytic perivascular cuffing with adjacent alveolar epithelial hyperplasia was noticed without an increased intraepithelial macrophage infiltrate and normal alveolar septal thickness in immunized macaques receiving 25 μg of S (Fig. 6F).

P.1 challenge recalls a broadly neutralizing anamnestic response and a variant-specific primary neutralizing response in naïve macaques

To better understand the immunological basis of events happening after late challenge, and to determine if P.1 challenge triggered an anamnestic response in immunized NHPs, post-challenge S-specific IgG concentrations and $PRNT_{50}$ titers were measured from sera collected upon necropsy at day 14. Late P.1 challenge significantly boosted serum IgG concentrations to levels attained at the post-immunization peak at Week 6, with less variance between animals, suggesting that a recall response was triggered by the heterologous infection (Fig. 7A).

Vaccine-matched (WA1/2020) and VOC neutralizing (i.e., B.1.351, P.1 and B.1.617) antibody levels were also all significantly boosted to levels attaining or surpassing the peak levels generated through initial immunization by 5-fold and upwards of 20-fold respectively (Fig. 7B and S2). Unsurprisingly, the greatest increase from pre-challenge neutralization was against the P.1 challenge isolate. Group A showed slightly higher P.1 NtAbs compared to Group B and C macaques and was the only group to have significantly higher titers across different variants. The lower degree of histopathology seen in Groups B and C may indicate that 25 µg S with either form of CoVaccine HT™ provides greater long-term protection. In Group D control macaques, P.1 challenge generated low levels of NtAbs compared to immunization alone, and it was only cross-reactive with the B.1.351 isolate and not to WA1/2020 nor B.1.617 isolates. This suggests that primary infection with one isolate of SARS-CoV-2 does not generate broad immunity against other variants in contrast to vaccine derived immunity, which is more broadly cross-reactive with VOCs, even months after peak immunity is observed.

DISCUSSION

Understanding the durability and breadth of vaccine-generated immunity is critical for predicting long-term protection during the COVID-19 pandemic and for informing policy on strategic resource deployment to facilitate equitable vaccine access. Diversifying the type of vaccines currently used beyond mRNA and viral vectors to include other vaccine platforms, such as protein subunit vaccines, can bolster global availability by mobilizing more thermostable vaccines to resource-poor areas, or overcoming anti-vector immunity and adverse effects, by using this platform as a booster to restore pre-existing natural or vaccine-induced immunity (*65-67*).

We have demonstrated that two doses of a subunit vaccine consisting of a prefusion S trimer (Wuhan-Hu-1) formulated with liquid or lyophilized CoVaccine HT™ reduces viral load and

provides sufficient, durable, cross-variant protection from mild to moderate disease lasting at least 3 months after the final boost. This supports previous findings in rhesus macaques that S trimer-based subunit protein vaccines are highly immunogenic and generate long-lasting, robust antibody responses (*68*). Furthermore, using a two-step purification method of immunoaffinity chromatography followed by a size-exclusion polishing step results in a homogenous antigen composition and reduces host-cell carryover plaguing conventional purification strategies for protein subunits (*69*). Also promising is the prospect that the adjuvant, CoVaccine HT™, can be lyophilized, and reconstituted simply with water for injection and still retain functionality. This technology has been previously used to develop mono- and multivalent filovirus vaccine formulations. Those studies demonstrated that single-vial, lyophilized formulations preserved the higher order antigen structure and the biophysical properties of the adjuvant (*70, 71*). Robust levels of S-specific IgG and homologous, as well as B.1.351, P.1 and B.1.617 cross-neutralizing antibodies, were detected throughout the extended study period and inversely correlate with viral load and lung damage. This report supports growing evidence that the Wuhan-Hu-1 S peptide sequence encoded by highly effective mRNA, viral vectored, and subunit protein vaccines, generates immunity that affords protection against circulating VOCs (*45, 46, 70-73*), even months after the final vaccine dose when antibody titers are waning. Furthermore, we noticed a few macaques receiving the higher antigen dose had developed increasingly potent cross-variant neutralizing titers immediately prior to viral challenge which were greater than titers observed during the peak humoral response. This suggests that a potentially remaining antigen depot or persistence of APC's may foster continued accumulation of somatic mutations and affinity maturation in memory B cells (*74, 75*) beyond the initial vaccination phase.

This study is also the first to describe the course of infection and histopathology of a SARS-CoV-2 P.1 infection in a NHP model. Consistent with what was described in WA1/2020 infected

313 cynomolgus macaques (*51, 52*), macaques challenged with the P.1 isolate did not develop
314 elevated temperature or decreased weight, nor did they show observable signs of respiratory
315 disease. Viral load in the upper and lower respiratory tract peaked early during infection two
316 days after challenge and gradually decreased to undetectable sgRNA levels by day 14 in
317 unprotected animals, similar to viral kinetics described in another study using the same
318 inoculating dose ($1x10^6$ $TCID_{50}$), but with an early pandemic isolate (*52*). Although P.1 is
319 estimated to be upwards of 2.4-fold more transmissible (*76*), it is unclear whether the higher
320 viral load observed during peak P.1 replication in this study compared to time-matched reports
321 for a non-variant isolate is a characteristic of P.1 replication or a discrepancy between readouts
322 from different RT-PCR procedures. However, we show that immunization with both 5 and 25 μg
323 doses of S effectively reduces viral load in both upper and lower respiratory tracts implying a
324 lower likelihood of viral transmission even in mildly symptomatic macaques. Histopathological
325 examination of lung and bronchial sections in unprotected macaques confirmed mild to
326 moderate disease, which was abrogated in immunized individuals. COVID-19 like disease
327 observed in this model consisted of increased intraalveolar and interstitial infiltration, as well as
328 giant syncytial cells, similar to previous observations (*51, 77, 78*). While both high and low
329 doses of S antigen generate statistically negligible differences in humoral responses during
330 peak immunity, it is clear from our findings that higher antigen doses, at least with CoVaccine
331 HT™ produces a more durable and protective response at this later timepoint.
332
333 Late P.1 challenge induced an anamnestic response in all immunized macaques that restored
334 S-specific antibody titers to peak serum concentrations seen shortly after the final boost, and
335 significantly enhanced vaccine-matched and VOC-neutralizing antibody titers. In most
336 macaques receiving 25 μg S, the immune recall occurred with little to no disease. The durability
337 and cross-variant neutralizing nature of immune responses generated by mRNA and viral
338 vectors has been documented up to six months or later (*79-82*). However, breakthrough

339 infections, particularly with variant strains, have been reported even in the presence of
340 detectable and high-level NtAbs (*54, 56, 59, 83*). Anamnestic responses in fully immunized
341 NHPs have been characterized previously with homologous and B.1.351 variant challenge and
342 agree with our observations that viral challenge boosts functional antibody levels. Our analysis
343 shows that viral challenge with a heterologous strain not only rapidly boosts homologous and
344 challenge strain specific NtAbs, but also NtAbs against the unencountered variants, B.1.351 and
345 B.1.617, underpinning the broad-spectrum potential of subunit protein vaccines. In contrast,
346 control macaques, receiving no S antigen, developed moderate levels of P.1 NtAbs that are only
347 cross-neutralizing with B.1.351, and barely neutralize WA1/2020 and B.1.617, suggesting that
348 natural infection with one strain of SARS-CoV-2 may confer only limited protection against other
349 VOCs. Of course, further affinity maturation could not be observed here as the study ended 14
350 days after challenge.
351
352 The small size of our treatment groups (n=3) is a limitation of our study and may therefore not
353 provide enough statistical power to strongly correlate antibody concentrations to viral load or
354 histopathology score. Furthermore, we cannot directly compare the outcome of our study to
355 other studies that evaluate vaccine efficacy soon after the final booster when immunity is
356 greatest, as vaccine efficacy is known to decline over time. Likewise, we could not benchmark
357 the efficacy of our vaccine formulation when the immunity is greatest at week 5, however, our
358 late challenge scheme accurately reflects the current urgent need for decisions about timing and
359 candidates for possible booster vaccinations during the pandemic situation as it provides useful
360 information regarding the real-life durability and breadth of vaccine protection. It furthermore
361 may shed light into the utility of protein vaccines to serve as prime or boost in combination with
362 other vaccines.
363

In conclusion, we show that a two-dose regimen of a prefusion-stabilized trimeric S subunit protein vaccine formulated with lyophilizable CoVaccine HT™ adjuvant reduces viral burden and high antigen doses can confer durable cross-variant immunity. Future efforts will therefore focus on developing a thermostabilized vaccine formulation in a single-vial presentation, potentially enabling facile worldwide distribution.

MATERIALS AND METHODS

Ethical Statement

The investigators adhered fully to the “Guide for the Care and Use of Laboratory Animals” by the Committee on Care of Laboratory Animal Resources Commission on Life Sciences, National Research Council. Cynomolgus macaques (*Macaca fascicularis*) were housed at BIOQUAL Inc. (Rockville, MD). All macaque experiments were reviewed and approved by BIOQUAL's Animal Care and Use Committee. BIOQUAL Inc. is accredited by the American Association for Accreditation of Laboratory Animal Care (AAALAC).

Study Design Cynomolgus macaque studies were performed using three adjuvanted vaccine formulations and an adjuvanted control using unrelated antigens: A) 5 µg of SARS-CoV-2 S protein with 10 mg lyophilized CoVaccine HT™, B) 25 µg S protein with 10 mg liquid CoVaccine HT™, C) 25 µg S protein with 10 mg lyophilized CoVaccine HT™, and D) 25 µg of Ebola Virus (EBOV) glycoprotein with 10 mg CoVaccine HT™, co-lyophilized in one vial. CoVaccine HT™ (BTG International Ltd, London, United Kingdom) was lyophilized as previously described (*71*) and reconstituted with sterile PBS before mixing with the antigen. Each group consisted of both male and female cynomolgus macaques (n = 3 for each formulation) weighing between 2.8 and 8.2 kg. Cynomolgus macaques of groups A-C were immunized intramuscularly (IM) in both deltoids (split dose) at weeks 0 and 3, control animals were immunized only once at week 0. Pre-challenge sera were collected at weeks 0, 3, 5, 6, 15. Challenge at week 15 with SARS-

CoV-2 P.1 variant, hCoV-19/Japan/TY7-501/2021, TY7-501 (BIOQUAL-generated stock [lot no. 031921-1215] in Calu-3 cells from seed stock no.TY7-501 was performed with an inoculum dose of $5x10^5$ $TCID_{50}$/mL administered to each animal in volumes of 1 mL by intratracheal and intranasal injection at each site. Nasal and oral swabs (NS and OS respectively) were collected on days 2, 4, 7, 10 and 14 after challenge. Bronchoalveolar lavage (BAL) samples were collected on days 2, 4, 7 and 10 after challenge. Necropsies and lung tissue collection were performed at the endpoint of the study at day 14 post-challenge. Samples were immediately processed and subsequently stored at −80°C prior to analysis. S-specific serum IgG concentrations were determined using a microsphere immunoassay (MIA; see below). NtAbs were measured using wild-type and rVSV-SARS-CoV-2 S PRNTs (see below). Viral load in the NS, OS and BAL was measured using plaque assays and quantification of genomic and subgenomic N transcript RNA (see below). Lung and bronchi tissues were processed, and H&E stained to delineate histopathological signs of disease in each animal.

Recombinant protein expression and purification

Plasmids were generated to express the pre-fusion, protease-resistant, trimeric transmembrane (TM)-deleted spike (S) glycoprotein from SARS-CoV-2 as described previously (*53*). Modifications to the gene include the removal of the furin and S2' cleavage site, the addition of 2 prolines between the heptad repeat 1 and central helix region, and a foldon trimerization domain. A stably transformed cell line was created by hygromycin B selection at 300 µg/mL. The cell line was scaled up to 1L using a WAVE bioreactor (Cytiva, Marlborough, MA) and induced with 200 µM $CuSO_4$.

Recombinant S protein was purified from clarified cell culture supernatants by immunoaffinity chromatography (IAC) using the SARS-CoV-2 cross-reactive mAb CR3022 (provided by Mapp Biopharmaceutical) coupled to NHS-activated Sepharose at a concentration of 10 mg/mL. The

antigen was eluted with a glycine buffer (pH 2) in tandem into a HiPrep 26/10 desalting column (Cytiva, Marlborough, MA) equilibrated with PBS. The oligomeric content was evaluated by size-exclusion chromatography using a HiLoad 16/600 column (GE Healthcare, Piscataway, NJ) equilibrated with PBS. The S protein eluted as a single peak and the final product migrated as two bands, corresponding to the monomer and trimer on SDS-PAGE, under denaturing conditions, and was reactive to CR3022 mAb on a western blot. Antigens were sterile filtered with a 0.22 µm syringe filter (Cytiva, Marlborough, MA) and stored at -80°C until use.

Analysis of antibodies by multiplex microsphere immunoassay (MIA)

The IgG antibody titers in sera were measured using a multiplex microsphere-based immunoassay as described previously (*53, 84-86*). Spectrally distinct, magnetic MagPlex® microspheres (Luminex Corporation, Austin, TX) were coupled to purified S, RBD or bovine serum albumin (BSA). A mixture of the antigen-coupled beads was incubated with sera diluted with PBS+ 1% BSA and 0.02% Tween 20 (PBS-BT) at 1:5,000 or 1:10,000 in black-sided 96-well plates for 3 hours at 37°C with agitation. Bound IgG was detected using 1µg/mL red phycoerythrin (R-PE)-conjugated goat anti-human IgG antibodies (Jackson ImmunoResearch, Inc., West Grove, PA) and resuspended in MAGPIX® drive fluid before being analyzed on a MAGPIX® Instrument (Luminex Corporation, Austin, TX).

To determine S-specific IgG concentrations in the sera, the median fluorescence intensity (MFI) readouts of each sample was interpolated against a standard curve generated using purified human IgG at concentrations in the range of 7.44 to 1000 ng/mL. To produce the antibody standard, IgG was purified from pooled sera of COVID-19 vaccinated human volunteers using protein A affinity chromatography, followed by immunoaffinity chromatography (IAC) using NHS-Sepharose (Cytiva, Marlborough, MA) coupled with recombinant S to select for S-specific IgG. Purity was assessed using SDS-PAGE and antibody concentration was quantified using UV_{280}

absorbance. The resulting MFI values were plotted against the Log_{10}-transformed concentrations and fitted using a sigmoidal dose-response, variable slope model (GraphPad Prism, San Diego, CA). The resulting curves yielded r^2 values > 0.99 with a well-defined top and bottom and the linear range of the curve. The experimental S-specific IgG concentrations in experimental samples were determined by interpolation on the standard curves, multiplied by the dilution factors and plotted as antibody concentrations (ng/mL).

Recombinant vesicular stomatitis virus (rVSV) neutralization assay

Replication-competent rVSV expressing SARS-CoV-2 S protein (Wuhan-Hu-1) was generated as described previously (*87*) and the virus stocks were amplified in Vero E6 cells. For the plaque reduction neutralization test (PRNT), individual NHP serum samples were heat-inactivated at 56°C for 30 minutes. Six 3-fold serial dilutions of serum samples, starting at 1:40 dilution, were prepared and incubated with 100 plaque-forming units (PFU) of rVSV-SARS-CoV-2-S at 37°C for 1 hour. Antibody-virus complexes were added to Vero cell monolayers in 6-well plates and incubated at 37°C for another hour followed by addition of overlay media mixed with 1% agarose. 72 hours later, cells were fixed and stained with a solution containing 1% formaldehyde, 1% methanol, and 0.05% crystal violet overnight for plaque enumeration. Neutralization titers ($PRNT_{50}$) were generated using a variable slope, nonlinear regression, with upper and lower constraints (100% and 0% neutralization, respectively), using Prism 9 (GraphPad Software, San Diego, CA).

$TCID_{50}$ and Wild-type SARS-CoV-2 virus $PRNT_{50}$ assay

$TCID_{50}$ and $PRNT_{50}$ assays were performed in a biosafety level 3 facility at BIOQUAL, Inc. (Rockville, MD). The $TCID_{50}$ assay was conducted by addition of 10-fold graded dilutions of samples to Vero TMPRSS2 cell monolayers. Serial dilutions were performed in the cell culture wells in quadruplicates. Positive (virus stock of known infectious titer in the assay) and negative

(medium only) control wells were included in each assay set-up. The plates were incubated at 37ºC, 5.0% CO2 for 4 days. The cell monolayers were visually inspected for CPE, i.e. complete destruction of the monolayer with cellular agglutination. The $TCID_{50}$ value was calculated using the Read-Muench formula (*88*). For samples which had less than 3 CPE positive wells, the $TCID_{50}$ could not be calculated using the Reed-Muench formula, and these samples were assigned a titer of below the limit of detection (i.e., <2.7 log10 $TCID_{50}$/mL). For optimal assay performance, the TCID50 value of the positive control should test within 2-fold of the expected value.

To measure neutralization, sera from each NHP were diluted to 1:10 followed by a 3 fold- serial dilution. Diluted samples were then incubated with 30 plaque-forming units of wild-type SARS-CoV-2 USA-WA1/2020 (BEI-NR-52281), B.1.351 (BEI NR-55282), or P.1. (BEI NR-54982) variants, in an equal volume of culture medium for 1 hour at 37°C. The serum-virus mixtures were added to a monolayer of confluent Vero E6 cells and incubated for one hour at 37°C in 5% CO_2. Each well was then overlaid with culture medium containing 0.5% methylcellulose and incubated for 3 days at 37°C in 5% CO_2. The plates were then fixed with methanol at -20°C for 30 minutes and stained with 0.2% crystal violet for 30 min at room temperature. $PRNT_{50}$ titers were calculated using a variable slope, nonlinear regression, with upper and lower constraints (100% and 0% neutralization, respectively), on Prism 9 (Graphpad Software, San Diego, CA).

Histopathology

NHP Lung tissue specimens from each lung lobe and bronchi were harvested at time of necropsy and preserved in 10% formalin before processing and parafilm embedded, fixed and stained with hematoxylin & eosin. For each NHP, one section from the bronchi and one section from each lobe on the right and left lung were selected for scoring, for a total of six sections. Pathologic findings on each slide were scored on a scale of 0 – 2 for intraalveolar edema, the

494 amount of BALT (bronchiolar-associated lymphoid tissue), and the presence of Interstitial
495 inflammation; and 0 – 3 for perivascular inflammatory infiltrates (cuffing), and intraalveolar
496 inflammation. (See Table S1.) Scores for the six slides from each macaque were tabulated, and
497 a cumulative average score was calculated for each NHP using a total of 30 scores as
498 replicates.
499
500 **SARS-CoV-2 Viral Genomic and subgenomic RNA quantitative RT-PCR**
501 The presence of viral RNA and viral replication in the BAL, NS, and OS after SARS-CoV-2 P.1
502 strain challenge was determined by quantitative RT-PCR. RNA was isolated from 200 µL
503 sample using the QIAamp MinElute Virus spin kit (Qiagen, Frederick, MD). For the qRT-PCR
504 assay, viral RNA was first isolated from BAL, NS and OS using the Qiagen MinElute virus spin
505 kit. To generate a control for the amplification reaction, RNA was isolated from the applicable
506 virus stock using the same procedure. The number of copies for the control were calculated
507 using known RNA weights per mol. A master mix was prepared containing Taq-polymerase,
508 obtained from the TaqMan RT-PCR kit (Bioline cat# BIO-78005), RT, RNAse inhibitor, a primer
509 pair at 2 µM concentration (2019-nCoV_N1-F: 5'-GAC CCC AAA ATC AGC GAA AT-3' and
510 2019-nCoV_N1-R: 5'-TCT GGT TAC TGC CAG TTG AAT CTG-3') and probe (2019-nCoV_N1-
511 P: 5'-FAM-ACC CCG CAT TAC GTT TGG TGG ACC-BHQ1-3') at a concentration of 2 µM. For
512 the reactions, 45 µL of the master mix and 5 µL of the sample RNA were added to the wells of a
513 96-well plate. All samples were tested in triplicate. Control RNA was prepared to contain 10^6 to
514 10^7 copies per 3 µL. Eight (8) 10-fold serial dilutions of control RNA were prepared and
515 produced a standard curve with a range of 1 to 10^7 copies/reaction. For amplification, the plate
516 was placed in an Applied Biosystems 7500 Sequence detector and amplified using the following
517 program: 48ºC for 30 minutes, 95ºC for 10 minutes followed by 40 cycles of 95ºC for 15
518 seconds, and 1 minute at 55ºC. Duplicate samples of each dilution were prepared as described
519 above. If the copy number exceeded the upper detection limit, the sample was diluted as

needed. The number of copies of RNA per mL was calculated by interpolation from the standard curve and multiplying by the reciprocal of 0.2 mL extraction volume. This gave a practical range of 50 to 5 x 10^8 RNA copies per mL for BAL samples and for nasal and oral swabs the viral loads were given per swab.

The RT-PCR assay for the sgRNA utilizes primers and a probe specifically designed to amplify and bind to a region of the N gene mRNA from the Coronavirus, which is not packaged into the virion. The signal was compared to a known standard curve of plasmid containing the sequence of part of the messenger RNA and calculated to give copies per ml. The control DNA was prepared to contain 10^7 copies. Seven 10-fold serial dilutions of control RNA were prepared using Buffer AVE and generated a standard curve with a range of 1 to 10^6 copies/reaction. Duplicate samples of each dilution were prepared as described above with the primer pair (SG-N-F: CGATCTCTTGTAGATCTGTTCTC and SG-N-R: GGTGAACCAAGACG CAGTAT) and probe (FAM- TAACCAGAATGGAGAACGCAGTGGG -BHQ). If the copy number exceeded the upper detection limit, the sample was diluted as needed. For amplification, the plate was placed in an Applied Biosystems 7500 Sequence detector and amplified using the following program: 48°C for 30 minutes, 95°C for 10 minutes followed by 40 cycles of 95°C for 15 seconds, and 1 minute at 55°C. The number of copies of RNA per ml was calculated by interpolation from the standard curve and multiplying by the reciprocal of 0.2 ml extraction volume. This gave a practical range of 50 to 5 x 10^7 RNA copies per mL for harvested samples.

Statistical analysis

Statistically significant differences between the geometric mean of IgG concentrations or MFI in groups given different vaccine formulations at each timepoint were determined using a two-way ANOVA followed by Dunnett's Multiple Comparison. Comparisons of $PRNT_{50}$ values between vaccine formulations was done using a Kruskal-Wallis Test followed by a Dunn's multiple

546 comparisons test. Correlations between IgG or PRNT titers to viral load in the BAL and NS was
547 examined using the non-parametric Spearman's correlation test. Differences between
548 histopathological scores in different treatment groups was calculated using a one-way ANOVA
549 followed by Dunnett's multiple comparison test with the cumulative scores of all slides per
550 macaque as replicates. All statistical analysis was completed using Graphpad Prism 9 software
551 (San Diego, CA).
552
553 **Supplementary Materials**
554 Fig. S1. Serum Wuhan-Hu-1 RBD-Specific IgG Kinetics
555 Fig S2. Pre-and Post-Challenge rVSV-SARS-CoV2-S Neutralizing Antibody Response
556 Fig S3. Individual $TCID_{50}$ Viral load from the BAL and NS
557 Fig S4. Individual Genomic Viral RNA Load
558 Fig S5. Individual Subgenomic N transcript RNA Load
559 Table S1 Detailed Histopathology Scoring System
560
561 **References:**

562 1. P. Zhou *et al.*, A pneumonia outbreak associated with a new coronavirus of probable bat
563 origin. *Nature* **579**, 270-273 (2020).
564 2. N. Zhu *et al.*, A Novel Coronavirus from Patients with Pneumonia in China, 2019. *The*
565 *New England journal of medicine* **382**, 727-733 (2020).
566 3. S. Garg *et al.*, Critical interpretative synthesis of herd immunity for COVID-19 pandemic.
567 *J Family Med Prim Care* **10**, 1117-1123 (2021).
568 4. C. Huang *et al.*, Clinical features of patients infected with 2019 novel coronavirus in
569 Wuhan, China. *Lancet* **395**, 497-506 (2020).
570 5. Z. Wu, J. M. McGoogan, Characteristics of and Important Lessons From the Coronavirus
571 Disease 2019 (COVID-19) Outbreak in China: Summary of a Report of 72314 Cases

From the Chinese Center for Disease Control and Prevention. *Jama* **323**, 1239-1242 (2020).

6. J. Helms *et al.*, Neurologic Features in Severe SARS-CoV-2 Infection. *The New England journal of medicine* **382**, 2268-2270 (2020).

7. M. Levi, J. Thachil, T. Iba, J. H. Levy, Coagulation abnormalities and thrombosis in patients with COVID-19. *Lancet Haematol* **7**, e438-e440 (2020).

8. R. Mao *et al.*, Manifestations and prognosis of gastrointestinal and liver involvement in patients with COVID-19: a systematic review and meta-analysis. *Lancet Gastroenterol Hepatol* **5**, 667-678 (2020).

9. S. Richardson *et al.*, Presenting Characteristics, Comorbidities, and Outcomes Among 5700 Patients Hospitalized With COVID-19 in the New York City Area. *Jama* **323**, 2052-2059 (2020).

10. Y. Bai *et al.*, Presumed Asymptomatic Carrier Transmission of COVID-19. *Jama* **323**, 1406-1407 (2020).

11. T. Ganyani *et al.*, Estimating the generation interval for coronavirus disease (COVID-19) based on symptom onset data, March 2020. *Euro Surveill* **25**, (2020).

12. X. He *et al.*, Temporal dynamics in viral shedding and transmissibility of COVID-19. *Nat Med* **26**, 672-675 (2020).

13. Z. He *et al.*, Seroprevalence and humoral immune durability of anti-SARS-CoV-2 antibodies in Wuhan, China: a longitudinal, population-level, cross-sectional study. *Lancet* **397**, 1075-1084 (2021).

14. F. J. Ibarrondo *et al.*, Rapid Decay of Anti-SARS-CoV-2 Antibodies in Persons with Mild Covid-19. *The New England journal of medicine* **383**, 1085-1087 (2020).

15. L. B. Rodda *et al.*, Functional SARS-CoV-2-Specific Immune Memory Persists after Mild COVID-19. *Cell* **184**, 169-183 e117 (2021).

16. D. S. Khoury *et al.*, Neutralizing antibody levels are highly predictive of immune protection from symptomatic SARS-CoV-2 infection. *Nat Med* **27**, 1205-1211 (2021).
17. J. Seow *et al.*, Longitudinal observation and decline of neutralizing antibody responses in the three months following SARS-CoV-2 infection in humans. *Nat Microbiol* **5**, 1598-1607 (2020).
18. A. K. Wheatley *et al.*, Evolution of immune responses to SARS-CoV-2 in mild-moderate COVID-19. *Nat Commun* **12**, 1162 (2021).
19. V. Gupta *et al.*, Asymptomatic reinfection in two healthcare workers from India with genetically distinct SARS-CoV-2. *Clin Infect Dis*, (2020).
20. D. Harrington *et al.*, Confirmed Reinfection with SARS-CoV-2 Variant VOC-202012/01. *Clin Infect Dis*, (2021).
21. D. Loconsole *et al.*, Symptomatic SARS-CoV-2 Reinfection in a Healthy Healthcare Worker in Italy Confirmed by Whole-Genome Sequencing. *Viruses* **13**, (2021).
22. B. Prado-Vivar *et al.*, A case of SARS-CoV-2 reinfection in Ecuador. *Lancet Infect Dis* **21**, e142 (2021).
23. R. L. Tillett *et al.*, Genomic evidence for reinfection with SARS-CoV-2: a case study. *Lancet Infect Dis* **21**, 52-58 (2021).
24. B. A. Johnson *et al.*, Loss of furin cleavage site attenuates SARS-CoV-2 pathogenesis. *Nature* **591**, 293-299 (2021).
25. J. A. Plante *et al.*, Spike mutation D614G alters SARS-CoV-2 fitness. *Nature* **592**, 116-121 (2021).
26. N. R. Faria *et al.*, Genomics and epidemiology of the P.1 SARS-CoV-2 lineage in Manaus, Brazil. *Science (New York, N.Y.)* **372**, 815-821 (2021).
27. P. Mlcochova *et al.*, SARS-CoV-2 B.1.617.2 Delta variant replication and immune evasion. *Nature*, (2021).

28. E. C. Sabino *et al.*, Resurgence of COVID-19 in Manaus, Brazil, despite high seroprevalence. *Lancet* **397**, 452-455 (2021).

29. FDA. (https://www.fda.gov/media/145802/download., 2021).

30. Z. Wang *et al.*, mRNA vaccine-elicited antibodies to SARS-CoV-2 and circulating variants. *Nature* **592**, 616-622 (2021).

31. T. T. Brehm *et al.*, SARS-CoV-2 Reinfection in a Healthcare Worker Despite the Presence of Detectable Neutralizing Antibodies. *Viruses* **13**, (2021).

32. C. M. Romano *et al.*, SARS-CoV-2 reinfection caused by the P.1 lineage in Araraquara city, Sao Paulo State, Brazil. *Rev Inst Med Trop Sao Paulo* **63**, e36 (2021).

33. M. S. D. Silva *et al.*, Early detection of SARS-CoV-2 P.1 variant in Southern Brazil and reinfection of the same patient by P.2. *Rev Inst Med Trop Sao Paulo* **63**, e58 (2021).

34. N. Zucman, F. Uhel, D. Descamps, D. Roux, J. D. Ricard, Severe reinfection with South African SARS-CoV-2 variant 501Y.V2: A case report. *Clin Infect Dis*, (2021).

35. T. Charmet *et al.*, Impact of original, B.1.1.7, and B.1.351/P.1 SARS-CoV-2 lineages on vaccine effectiveness of two doses of COVID-19 mRNA vaccines: Results from a nationwide case-control study in France. *Lancet Reg Health Eur* **8**, 100171 (2021).

36. M. Imai *et al.*, Characterization of a new SARS-CoV-2 variant that emerged in Brazil. *Proceedings of the National Academy of Sciences of the United States of America* **118**, (2021).

37. P. Wang *et al.*, Increased resistance of SARS-CoV-2 variant P.1 to antibody neutralization. *Cell host & microbe* **29**, 747-751 e744 (2021).

38. FDA. (Food and Drug Administration https://www.fda.gov/emergency-preparedness-and-response/coronavirus-disease-2019-covid-19/pfizer-biontech-covid-19-vaccine., 2021), vol. 2021.

646 39. FDA. (U.S, Food and Drug Administration, https://www.fda.gov/emergency-
647 preparedness-and-response/coronavirus-disease-2019-covid-19/moderna-covid-19-
648 vaccine., 2021), vol. 2021.
649 40. FDA. (Food and Drug Administration, https://www.fda.gov/news-events/press-
650 announcements/fda-issues-emergency-use-authorization-third-covid-, 2021), vol. 2021.
651 41. L. A. Jackson *et al.*, An mRNA Vaccine against SARS-CoV-2 - Preliminary Report. *The*
652 *New England journal of medicine* **383**, 1920-1931 (2020).
653 42. F. P. Polack *et al.*, Safety and Efficacy of the BNT162b2 mRNA Covid-19 Vaccine. *The*
654 *New England journal of medicine* **383**, 2603-2615 (2020).
655 43. J. Sadoff *et al.*, Safety and Efficacy of Single-Dose Ad26.COV2.S Vaccine against
656 Covid-19. *The New England journal of medicine*, (2021).
657 44. S. A. Madhi *et al.*, Efficacy of the ChAdOx1 nCoV-19 Covid-19 Vaccine against the
658 B.1.351 Variant. *The New England journal of medicine* **384**, 1885-1898 (2021).
659 45. V. Shinde *et al.*, Efficacy of NVX-CoV2373 Covid-19 Vaccine against the B.1.351
660 Variant. *The New England journal of medicine* **384**, 1899-1909 (2021).
661 46. P. Jalkanen *et al.*, COVID-19 mRNA vaccine induced antibody responses against three
662 SARS-CoV-2 variants. *Nat Commun* **12**, 3991 (2021).
663 47. J. Liu *et al.*, BNT162b2-elicited neutralization of B.1.617 and other SARS-CoV-2
664 variants. *Nature*, (2021).
665 48. A. Muik *et al.*, Neutralization of SARS-CoV-2 lineage B.1.1.7 pseudovirus by BNT162b2
666 vaccine-elicited human sera. *Science (New York, N.Y.)* **371**, 1152-1153 (2021).
667 49. P. Supasa *et al.*, Reduced neutralization of SARS-CoV-2 B.1.1.7 variant by
668 convalescent and vaccine sera. *Cell* **184**, 2201-2211 e2207 (2021).
669 50. L. A. Hilgers, A. G. Blom, Sucrose fatty acid sulphate esters as novel vaccine adjuvant.
670 *Vaccine* **24 Suppl 2**, S2-81-82 (2006).

51. F. J. Salguero *et al.*, Comparison of rhesus and cynomolgus macaques as an infection model for COVID-19. *Nat Commun* **12**, 1260 (2021).

52. B. Rockx *et al.*, Comparative pathogenesis of COVID-19, MERS, and SARS in a nonhuman primate model. *Science (New York, N.Y.)* **368**, 1012-1015 (2020).

53. C. Y. Lai *et al.*, Recombinant protein subunit SARS-CoV-2 vaccines formulated with CoVaccine HT adjuvant induce broad, Th1 biased, humoral and cellular immune responses in mice. *bioRxiv : the preprint server for biology*, (2021).

54. A. Baj *et al.*, Breakthrough Infections of E484K-Harboring SARS-CoV-2 Delta Variant, Lombardy, Italy. *Emerging infectious diseases* **27**, (2021).

55. M. Bergwerk *et al.*, Covid-19 Breakthrough Infections in Vaccinated Health Care Workers. *The New England journal of medicine*, (2021).

56. E. Hacisuleyman *et al.*, Vaccine Breakthrough Infections with SARS-CoV-2 Variants. *The New England journal of medicine* **384**, 2212-2218 (2021).

57. I. Kroidl *et al.*, Vaccine breakthrough infection and onward transmission of SARS-CoV-2 Beta (B.1.351) variant, Bavaria, Germany, February to March 2021. *Euro Surveill* **26**, (2021).

58. T. Kustin *et al.*, Evidence for increased breakthrough rates of SARS-CoV-2 variants of concern in BNT162b2-mRNA-vaccinated individuals. *Nat Med* **27**, 1379-1384 (2021).

59. N. Vignier *et al.*, Breakthrough Infections of SARS-CoV-2 Gamma Variant in Fully Vaccinated Gold Miners, French Guiana, 2021. *Emerging infectious diseases* **27**, (2021).

60. C. M. Brown *et al.*, Outbreak of SARS-CoV-2 Infections, Including COVID-19 Vaccine Breakthrough Infections, Associated with Large Public Gatherings - Barnstable County, Massachusetts, July 2021. *MMWR Morb Mortal Wkly Rep* **70**, 1059-1062 (2021).

61. M. D. Fahlberg *et al.*, Cellular events of acute, resolving or progressive COVID-19 in SARS-CoV-2 infected non-human primates. *Nat Commun* **11**, 6078 (2020).

62. M. Guebre-Xabier *et al.*, NVX-CoV2373 vaccine protects cynomolgus macaque upper and lower airways against SARS-CoV-2 challenge. *Vaccine* **38**, 7892-7896 (2020).

63. C. Woolsey *et al.*, Establishment of an African green monkey model for COVID-19. *bioRxiv : the preprint server for biology*, (2020).

64. M. Bergwerk *et al.*, Covid-19 Breakthrough Infections in Vaccinated Health Care Workers. *The New England journal of medicine*, (2021).

65. A. M. Chmielewska *et al.*, Combined adenovirus vector and hepatitis C virus envelope protein prime-boost regimen elicits T cell and neutralizing antibody immune responses. *Journal of virology* **88**, 5502-5510 (2014).

66. J. A. Choi *et al.*, Cross-Protection against MERS-CoV by Prime-Boost Vaccination Using Viral Spike DNA and Protein. *Journal of virology* **94**, (2020).

67. S. C. Gilbert, T. Lambe, Recombinant protein vaccines against SARS-CoV-2. *Lancet Infect Dis*, (2021).

68. M. Mandolesi *et al.*, SARS-CoV-2 protein subunit vaccination of mice and rhesus macaques elicits potent and durable neutralizing antibody responses. *Cell Rep Med* **2**, 100252 (2021).

69. P. A. Goepfert *et al.*, Safety and immunogenicity of SARS-CoV-2 recombinant protein vaccine formulations in healthy adults: interim results of a randomised, placebo-controlled, phase 1-2, dose-ranging study. *Lancet Infect Dis*, (2021).

70. K. B. Preston *et al.*, Preservation of Quaternary Structure in Thermostable, Lyophilized Filovirus Glycoprotein Vaccines: A Search for Stability-Indicating Assays. *J Pharm Sci* **109**, 3716-3727 (2020).

71. K. B. Preston *et al.*, Single-vial filovirus glycoprotein vaccines: Biophysical characteristics and immunogenicity after co-lyophilization with adjuvant. *Vaccine*, (2021).

72. G. Alter *et al.*, Immunogenicity of Ad26.COV2.S vaccine against SARS-CoV-2 variants in humans. *Nature*, (2021).

73. M. G. Joyce *et al.*, Efficacy of a Broadly Neutralizing SARS-CoV-2 Ferritin Nanoparticle Vaccine in Nonhuman Primates. *bioRxiv : the preprint server for biology*, (2021).

74. J. N. Purushotham, N. van Doremalen, V. J. Munster, SARS-CoV-2 vaccines: anamnestic response in previously infected recipients. *Cell Res* **31**, 827-828 (2021).

75. K. G. Sprenger, J. E. Louveau, P. M. Murugan, A. K. Chakraborty, Optimizing immunization protocols to elicit broadly neutralizing antibodies. *Proceedings of the National Academy of Sciences of the United States of America* **117**, 20077-20087 (2020).

76. N. R. Faria *et al.*, Genomics and epidemiology of a novel SARS-CoV-2 lineage in Manaus, Brazil. *medRxiv*, (2021).

77. B. Salzberger *et al.*, Epidemiology of SARS-CoV-2. *Infection* **49**, 233-239 (2021).

78. J. Yu *et al.*, Protective efficacy of Ad26.COV2.S against SARS-CoV-2 B.1.351 in macaques. *Nature* **596**, 423-427 (2021).

79. D. H. Barouch *et al.*, Durable Humoral and Cellular Immune Responses Following Ad26.COV2.S Vaccination for COVID-19. *medRxiv*, (2021).

80. R. R. Goel *et al.*, mRNA Vaccination Induces Durable Immune Memory to SARS-CoV-2 with Continued Evolution to Variants of Concern. *bioRxiv : the preprint server for biology*, (2021).

81. A. Pegu *et al.*, Durability of mRNA-1273 vaccine-induced antibodies against SARS-CoV-2 variants. *Science (New York, N.Y.)*, (2021).

82. A. T. Widge *et al.*, Durability of Responses after SARS-CoV-2 mRNA-1273 Vaccination. *The New England journal of medicine* **384**, 80-82 (2021).

83. N. E. Blachere, E. Hacisuleyman, R. B. Darnell, Vaccine Breakthrough Infections with SARS-CoV-2 Variants. Reply. *The New England journal of medicine* **385**, e7 (2021).

748 84. B. K. Haun *et al.*, CoVaccine HT adjuvant potentiates robust immune responses to
749 recombinant SARS-CoV-2 Spike S1 immunisation. *bioRxiv : the preprint server for*
750 *biology*, (2020).
751 85. A. To *et al.*, Recombinant Zika Virus Subunits Are Immunogenic and Efficacious in Mice.
752 *mSphere* **3**, (2018).
753 86. M. Namekar, M. Kumar, M. O'Connell, V. R. Nerurkar, Effect of serum heat-inactivation
754 and dilution on detection of anti-WNV antibodies in mice by West Nile virus E-protein
755 microsphere immunoassay. *PloS one* **7**, e45851 (2012).
756 87. W. Furuyama *et al.*, Rapid protection from COVID-19 in nonhuman primates vaccinated
757 intramuscularly but not intranasally with a single dose of a recombinant vaccine. *bioRxiv*
758 *: the preprint server for biology*, (2021).
759 88. L. J. Reed, H. Muench, A simple method of estimating fifty percent end points. *American*
760 *journal of epidemiology* **27**, 493-497 (1938).
761

762 **Acknowledgements:** We would like to thank Takaji Wakita, from the National Institute of
763 Infectious Diseases, Japan, for the P.1 viral challenge strain, and Shelby O'Connor and John
764 Baczenas from the University of Wisconsin-Madison, USA, for deep sequencing our inhouse
765 viral stock. We also would like to thank Adrian Creanga from the Vaccine Research Center-
766 NIAID, USA for the Vero TMPRSS2 cell line used in our $TCID_{50}$ and $PRNT_{50}$ assays, as well as
767 Andrea Marzi, Laboratory of Virology, NIAID-NIH, USA, for the rVSV-SARS-CoV 2 virus stock
768 used in our surrogate $PRNT_{50}$ assay. Furthermore, we would like to thank Melissa Hamilton, the
769 study coordinator at Bioqual Inc., USA; Mapp Biopharmaceutical Inc, for the CR3022 mAb used
770 for protein purification; BTG International Limited for the CoVaccine HT^{TM} adjuvant, and Miyoko
771 Bellinger and Kristen Ewall from the JABSOM Histocore for preparing lung tissue sections for
772 histopathological analysis.
773

774 **Funding:** This work was supported by:

775 National Institute of Allergy and Infectious Diseases Grant R01AI132323 (ATL)

776 National Institute of Minority Health and Health Disparities Grant U54MD007601 (JRH)

777 National Institute of General Medical Sciences Grant P30GM114737 (RY)

778 Institutional funds from University of Hawai‘i at Mānoa, BIOQUAL Inc. and Soligenix Inc.

779

780 **Author Contribution:**

781 Conceptualization: AT, MML, HA, OD, ATL

782 Methodology: AT, TSW, KT, LP, HA, CYL, ATL

783 Investigation: AT, TSW, KT, LP, JG, ND, AC, BN, ZF, AVR, JYO

784 Formal Analysis: AT, MML, KT, ATL

785 Visualization: AT, KT

786 Funding acquisition: OD, ATL

787 Project administration: HA, OD, ATL

788 Supervision: HA, OD, ATL

789 Writing – original draft: AT, KT, ATL

790 Writing – review & editing: AT, TSW, MML, KT, HA, OD, ATL

791

792 **Competing Interests:**

793 ATL and OD are named inventors on a patent application covering a recombinant subunit

794 vaccine for SARS-CoV-2. LP, JG, ND, AC, BN, ZF, AVR, JYO and HA are current employees of

795 BIOQUAL, Inc. OD is a current employee of Soligenix Inc. All other authors declare no

796 competing interests.

797

798 **Data and material availability:** All data are available in the main text or the supplementary

799 materials

800

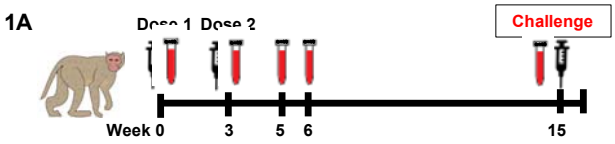

Group	Antigen Dose	Adjuvant Dose	Adjuvant State	N	Symbol
A	5 µg Spike	10 µg CoVaccine HT™	Lyophilized	3	●
B	25 µg Spike	10 µg CoVaccine HT™	Liquid	3	■
C	25 µg Spike	10 µg CoVaccine HT™	Lyophilized	3	▲
D	25 ug unrelated antigen	10 µg CoVaccine HT™	Lyophilized	3	◇

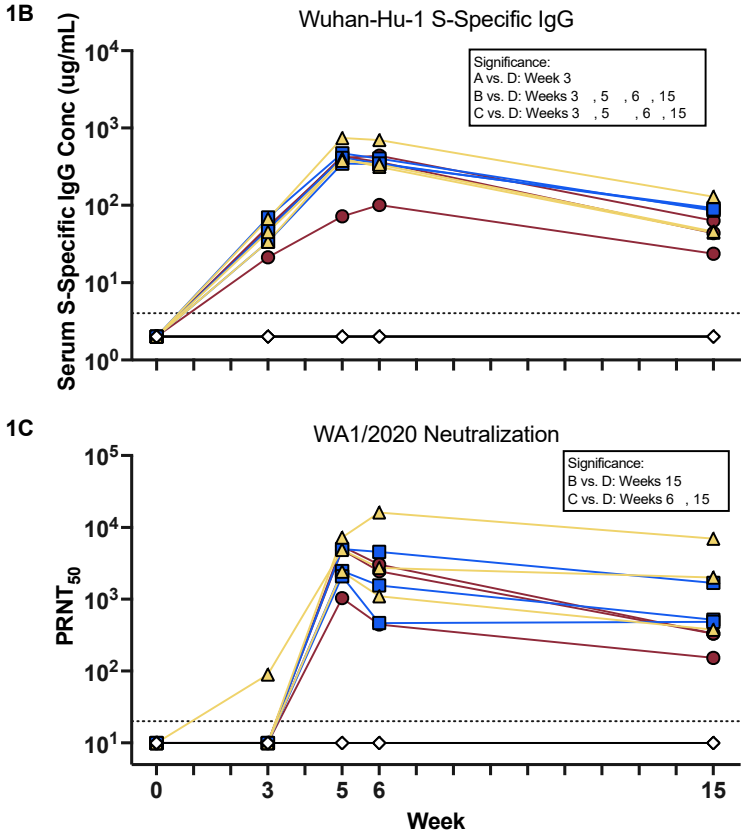

Figure 1. Vaccine Scheme, IgG and Neutralizing Antibody Kinetics ((A) 12 cynomolgus macaques were separated into 4 groups and given either 5 or 25 µg S protein formulated with either liquid or reconstituted, lyophilized CoVaccine HT™ adjuvant. Two doses were administered IM 3 weeks apart and sera was collected at indicated time points. Macaques were challenged IN and IT with a total of $1x10^6$ $TCID_{50}$ of the SARS-CoV-2 P.1 strain. (B) Serum Wuhan-Hu-1 S-specific IgG kinetics measured using a MIA with purified, human S-specific IgG standards to estimate serum concentration. Dashed line indicates the limit of quantification (LOQ, ≤4 µg/mL). Individual values falling below the LOQ were set to ½ LOQ. Significance was calculated using a one-way ANOVA followed by a Dunnett's Multiple Comparison to Group D at each time point. (C) WA1/2020 neutralizing antibody kinetics were measured using a WT SARS-CoV-2 PRNT assay. Curve-fitted $PRNT_{50}$ titers were calculated using a sigmoidal dose response curve. Dashed line indicates the limit of detection (LOD, ≤1:20). Individual values falling below the LOD were set to ½ LOD. Significance was calculated using a Kruskal-Wallis Test followed by a Dunn's Multiple Comparison. (*p≤0.05, **p≤0.01).

801

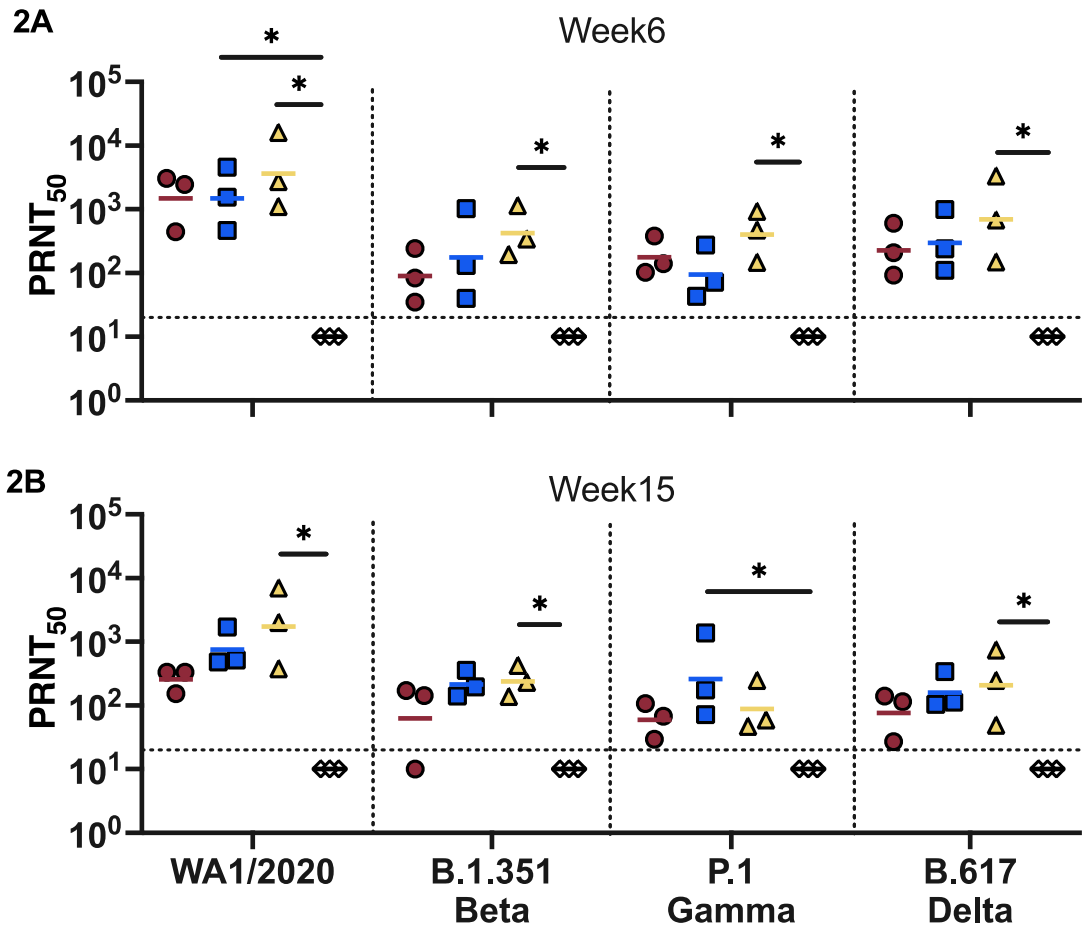

Figure 2. Cross-Neutralizing Antibody Titers Neutralizing antibody titers at (A) week 6 and (B) week 15 were measured using a WT SARS-CoV-2 PRNT assay with the WA1/2020, B.1.351 (Beta), P.1 (Gamma), B.1.617 (Delta) VOC. Curve-fitted $PRNT_{50}$ titers were calculated using a sigmoidal dose response curve. Dashed line indicates the LOD (≤1:20). Individual values falling below the LOD were set to ½ LOD. Significance was calculated using a Kruskal-Wallis Test followed by a Dunn's Multiple Comparison to Group D at each time point. Horizontal bars mark the GMT of each group (*p≤0.05).

802

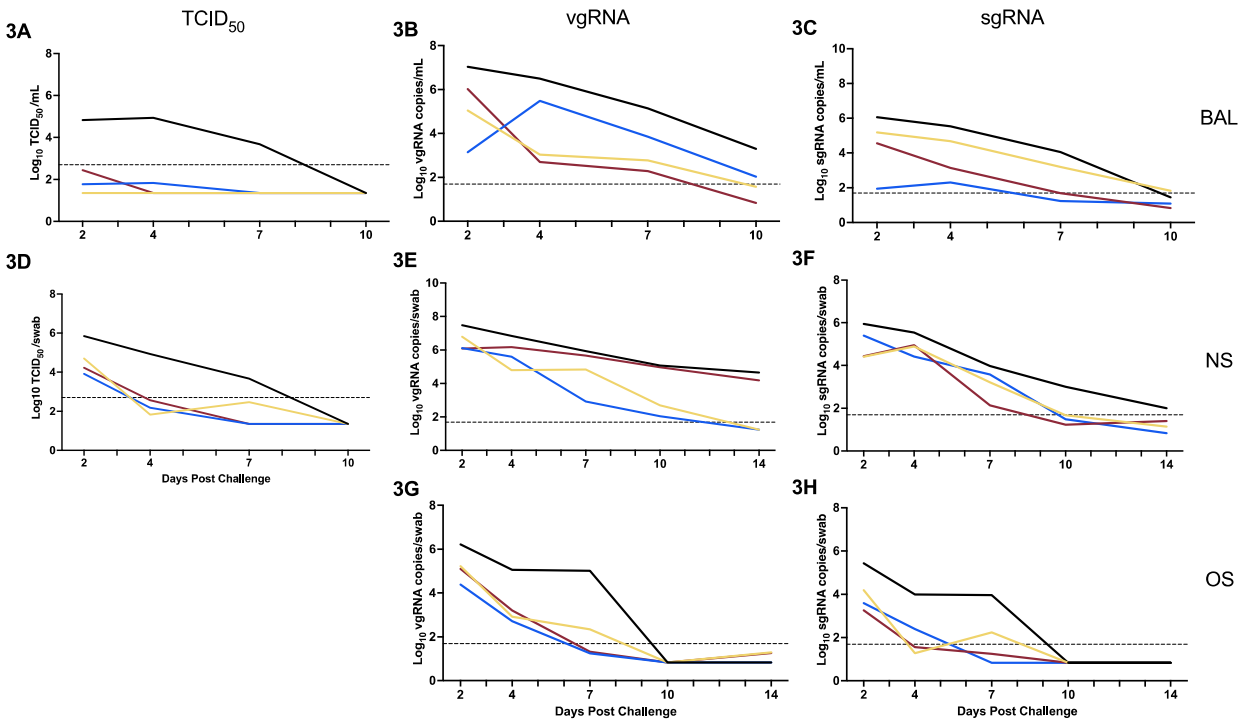

Figure 3. Viral Load Kinetics after P.1 Challenge GMT of the (A & D) $TCID_{50}$ titers; (B, E, G) viral genomic; and (C, F, H) subgenomic N RNA copies from the (A, B, C) bronchoalveolar lavage (BAL); (D, E, F) nasal swab (NS); and (G, H) oral swab (OS) collected at the time points indicated. Dashed line indicates the assay-specific LOD. Individual values falling below the LOD were set to ½ LOD.

803

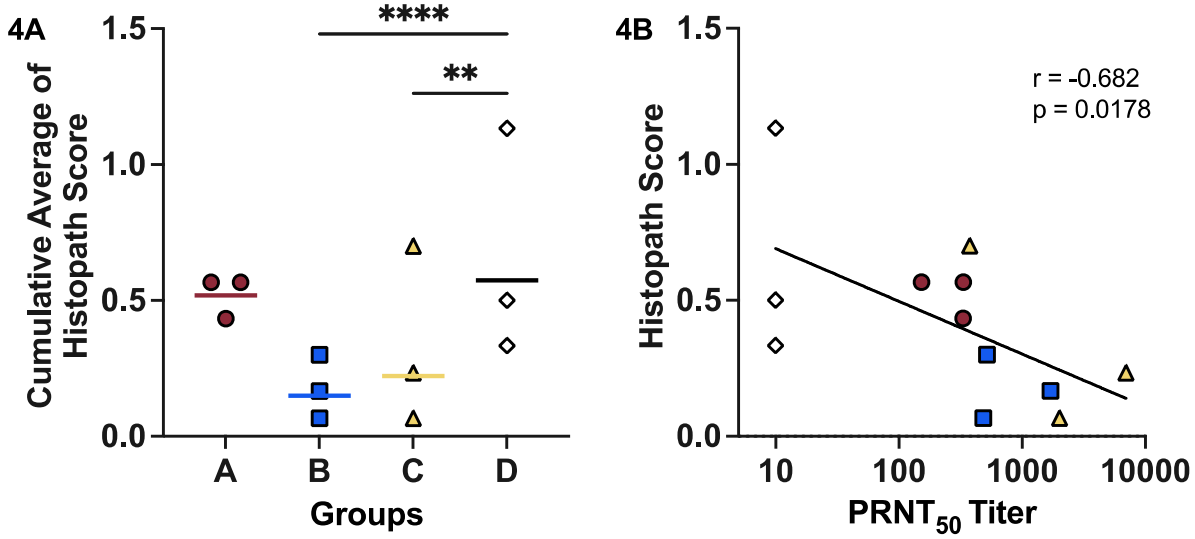

Figure 4. Histopathology Score and Correlation with Neutralizing Antibodies (A) Cumulative average histopathology score was determined by averaging the scores of six sections cut from each lobe and the bronchi. The presence and severity of edema, intra-alveolar inflammation, perivascular cuffing, increased BALT and interstitial inflammation was determined and assigned scores ranging from 0-3. Significant differences in lung histopathology were calculated using a one-way ANOVA followed by a Dunnett's multiple comparison to Group D with the scores from each section (30 scores per macaque) as replicates. Horizontal bars mark the GMT of each group. (**p≤0.01, ****p≤0.0001) (B) Correlation between histopathology scores and WA1/2020-specific $PRNT_{50}$ titers were determine using a Spearman's correlation test.

804

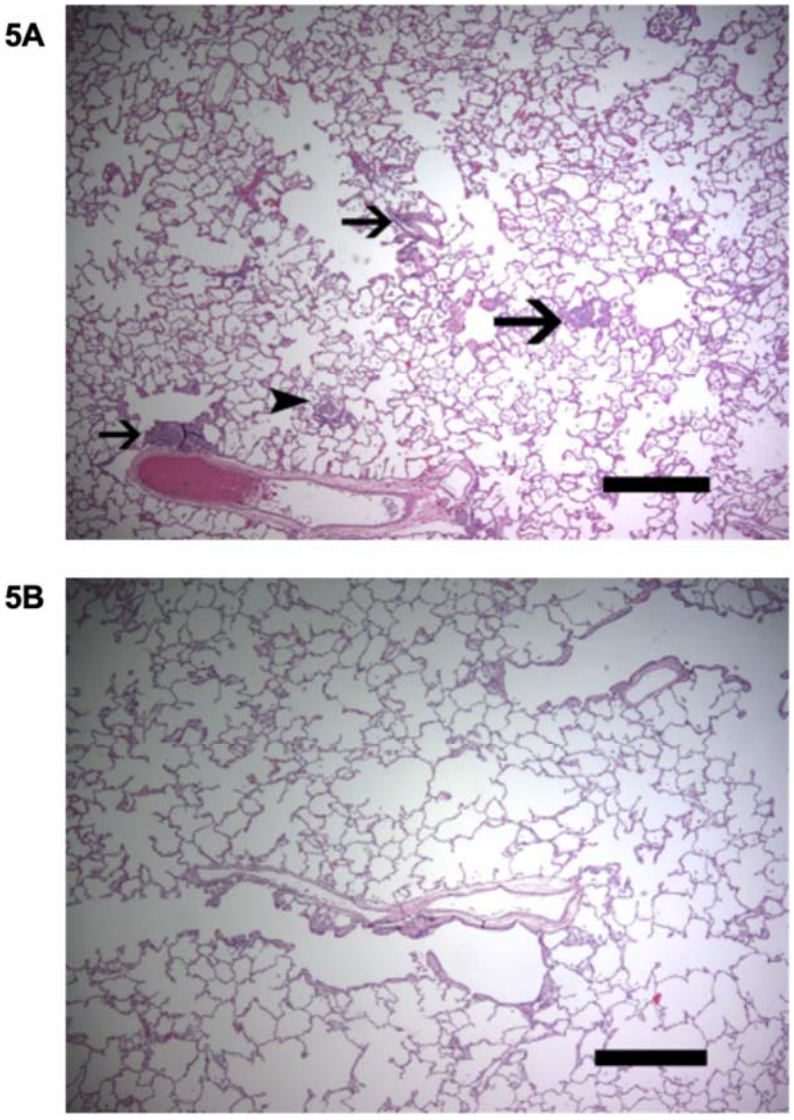

Figure 5 Histopathology observed in Hematoxylin and Eosin-Stained Lung Sections of Control Cynomolgus Macaques Compared to Immunized Macaques after P.1 challenge (A) Representative low power view of a lung section showing distribution of lymphocytic perivascular cuffing (arrows) and clusters of intraalveolar macrophages (arrowhead) in an unprotected macaque. (B) Representative low power view of a lung section from an immunized macaque which did not exhibit pathologic changes. Scale Bar = 500 microns.

805

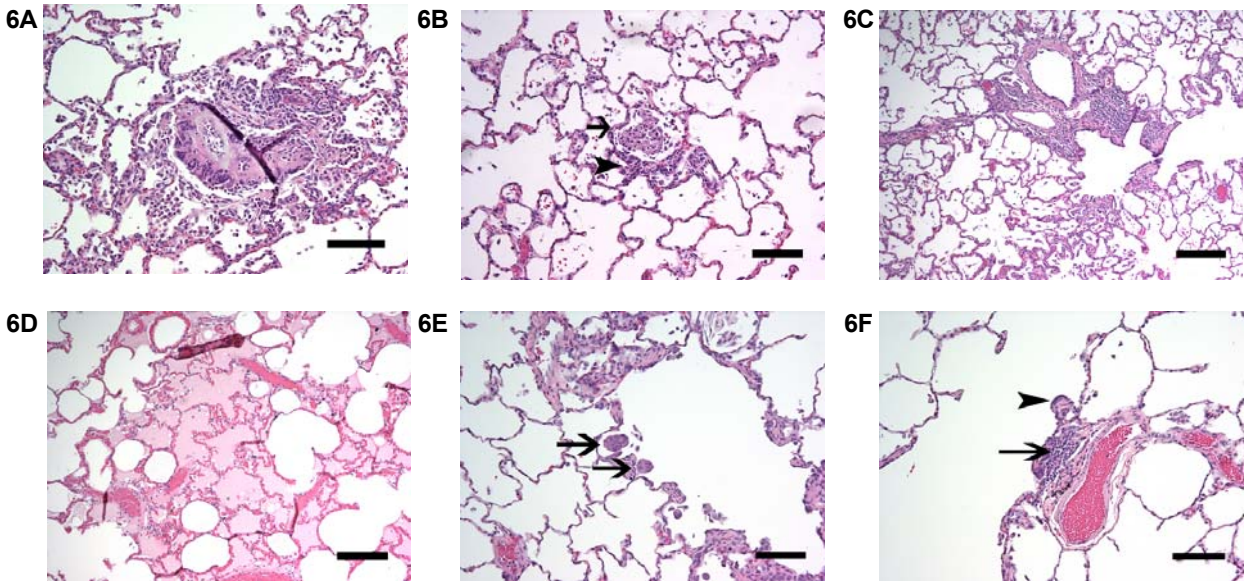

Figure 6 Histopathology Observed in Control Cynomolgus Macaques Compared to that Observed in Immunized Macaques after P.1 Challenge (A-D) unprotected macaques. (A) A syncytium of intraalveolar multinucleated giant cells is seen surrounded by an acute and eosinophilic inflammatory infiltrate. (B) Increased intraalveolar macrophages and an intraalveolar multinucleated giant cell accompanied by interstitial lymphocytic inflammation and thickening. (C) Complete lymphocytic perivascular cuffing with increased intra-alveolar macrophages. (D) Proteinaceous edema fluid in alveolar spaces. (E-F) Protected macaques. (E) Intraalveolar multinucleated giant cells (arrows) without increased intraalveolar macrophages, lymphocytic vascular cuffing or interstitial inflammation. (F) Partial lymphocytic perivascular cuff (arrow) with adjacent alveolar epithelial hyperplasia (arrowhead) without alveolar septal thickening. Scale bar = 10 microns.

806

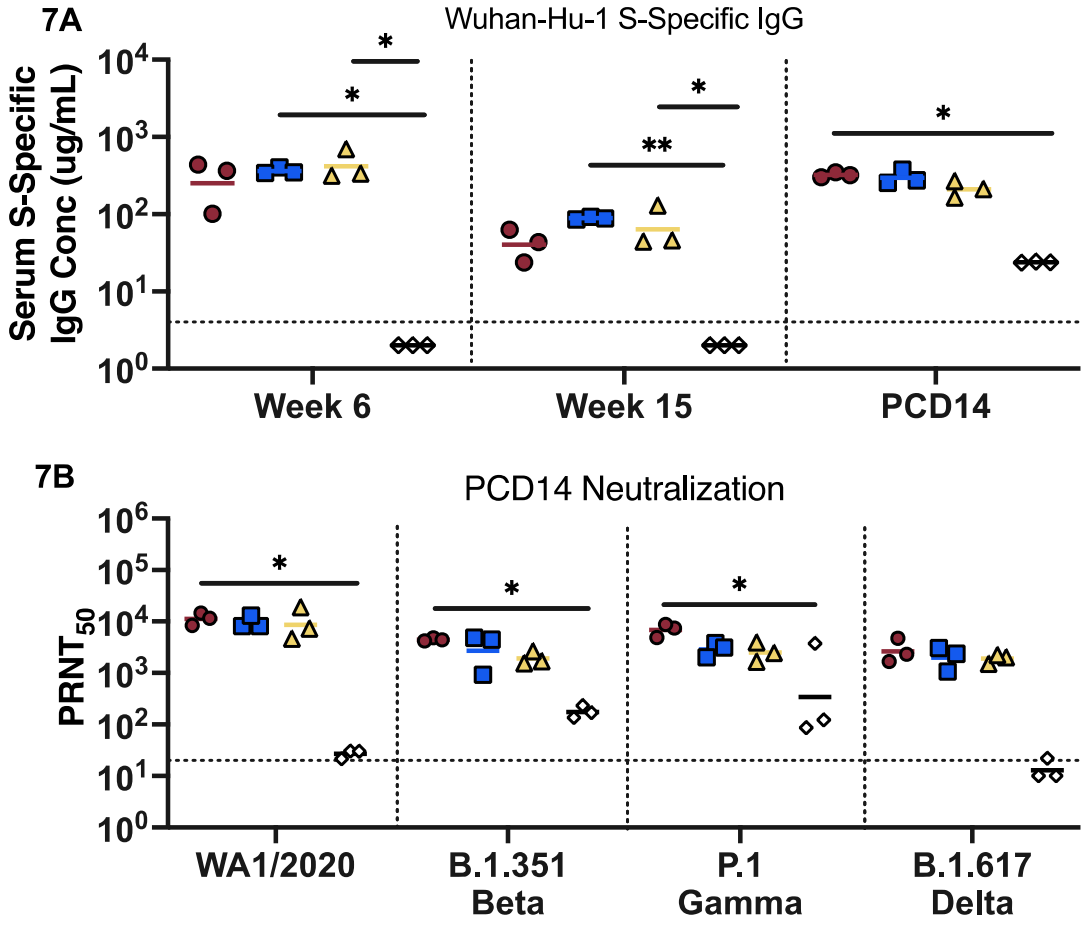

Figure 7. Post-Challenge Anamnestic Response (A) Vaccine-matched S-specific IgG conc. from sera collected at week 6, week 15 and at 14-days post-challenge, measured by MIA. IgG concentrations were estimated using a human S-specific IgG standard as described previously. Horizonal bars mark the GMT for each group. Dashed line indicates the LOQ (≤4 µg/mL) Individual values falling below the LOQ were set to ½ LOQ (B) Neutralizing antibodies 14 days after P.1 challenge were measured using a WT SARS-CoV-2 PRNT assay with the WA1/2020, B.1.351 (Beta), P.1 (Gamma), B.1.617 (Delta) VOC. Curve-fitted $PRNT_{50}$ titers were calculated using a sigmoidal dose response curve. Dashed line indicates the LOD (≤1:20). Individual values falling below the LOD were set to ½ LOD. Significance was calculated using a Kruskal-Wallis Test followed by a Dunn's Multiple Comparison to Group D at each time point. (*p≤0.05, **p≤0.01).